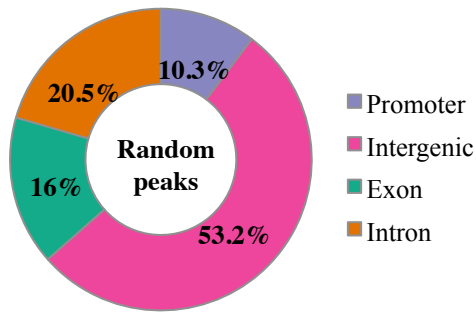
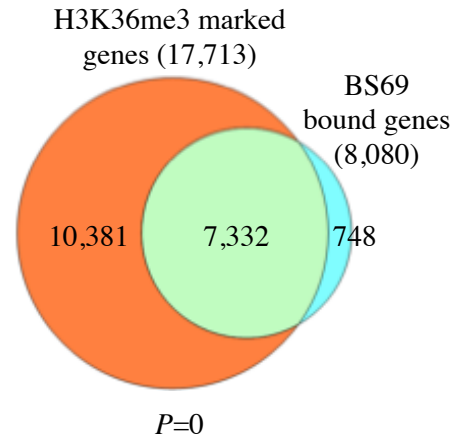


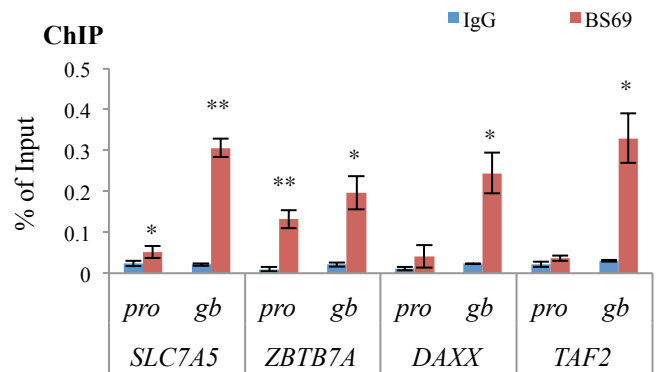
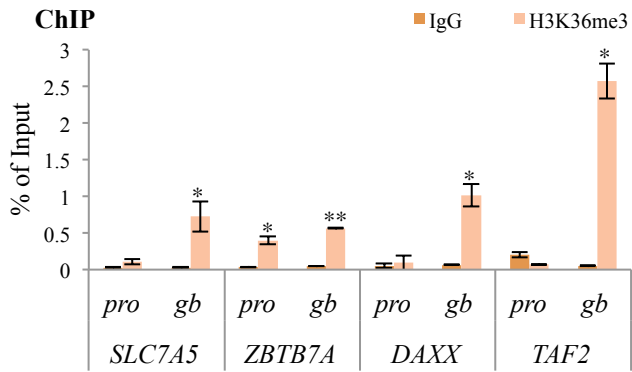
A



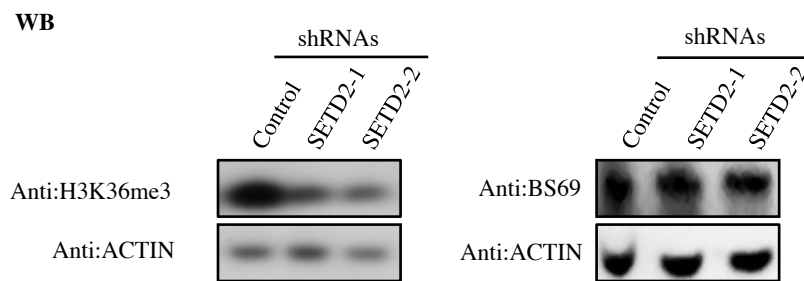
B



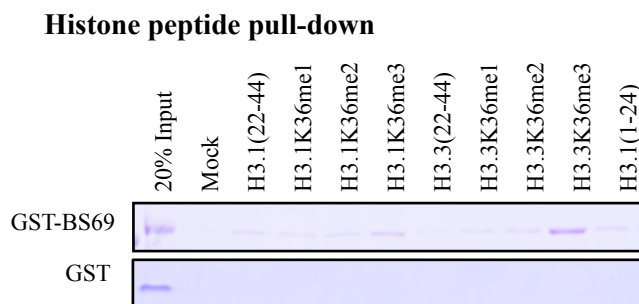
C



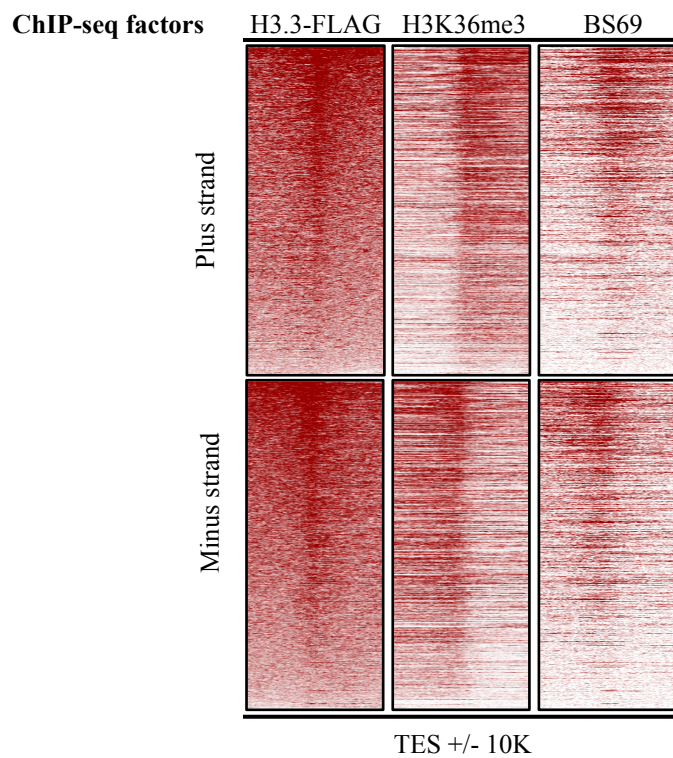
D



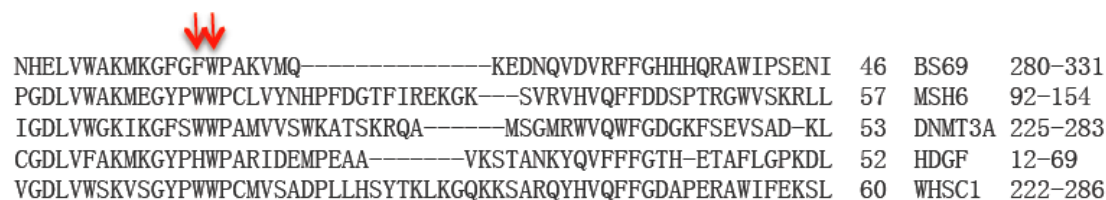
A



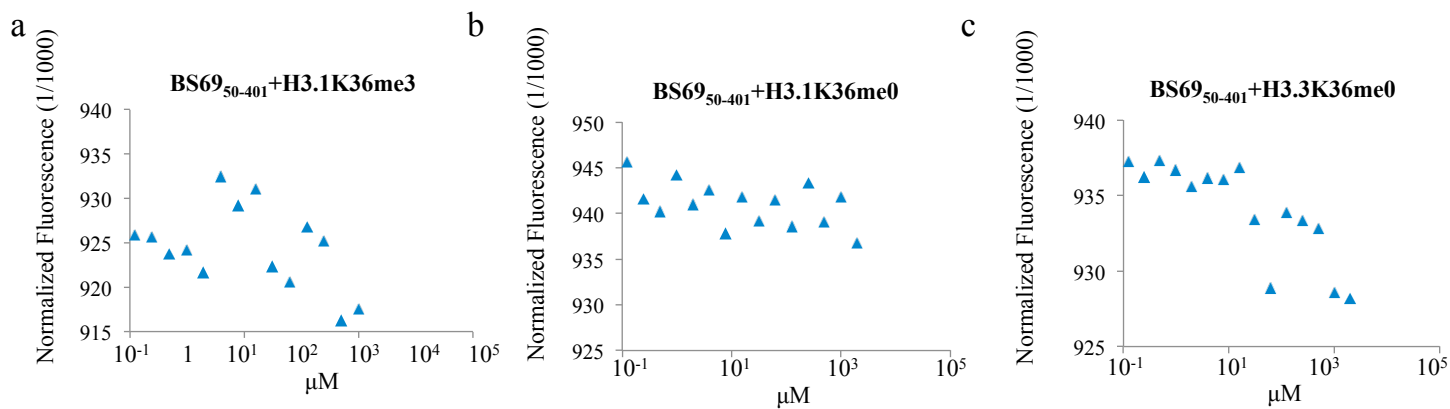
B



C

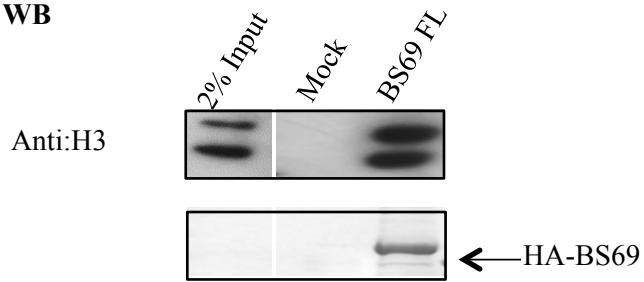


D



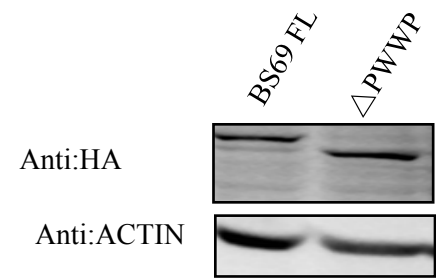
E

WB



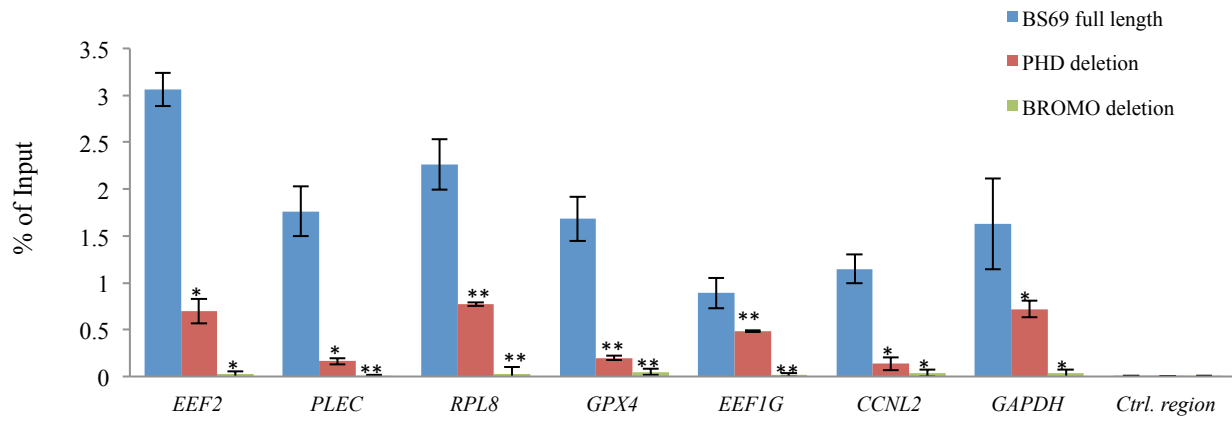
F

WB

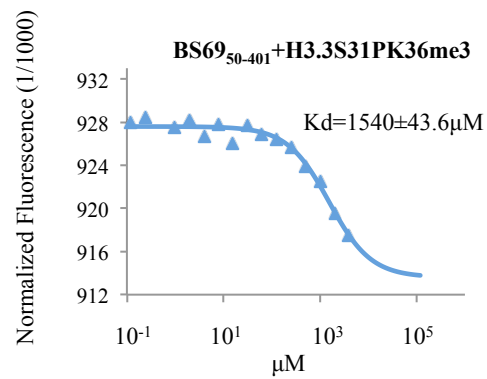


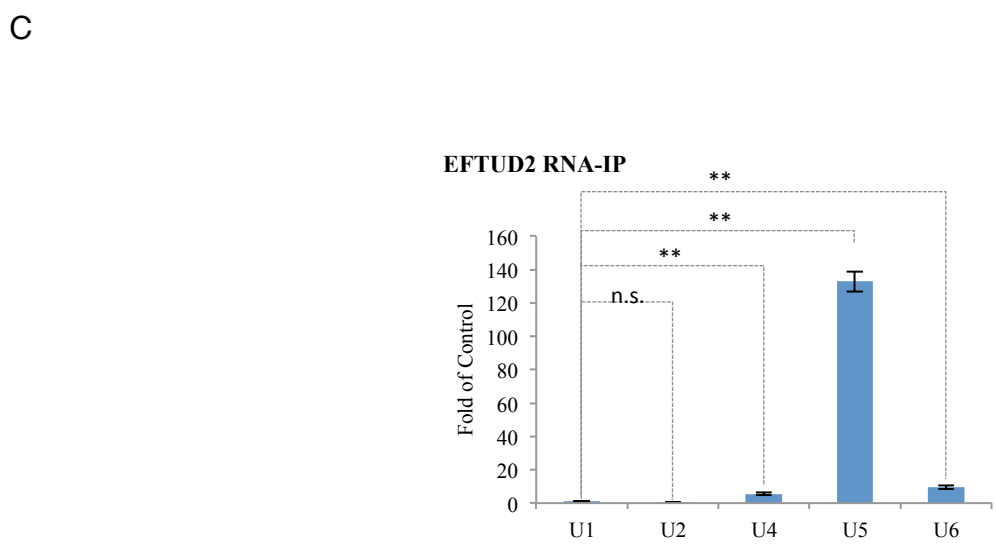
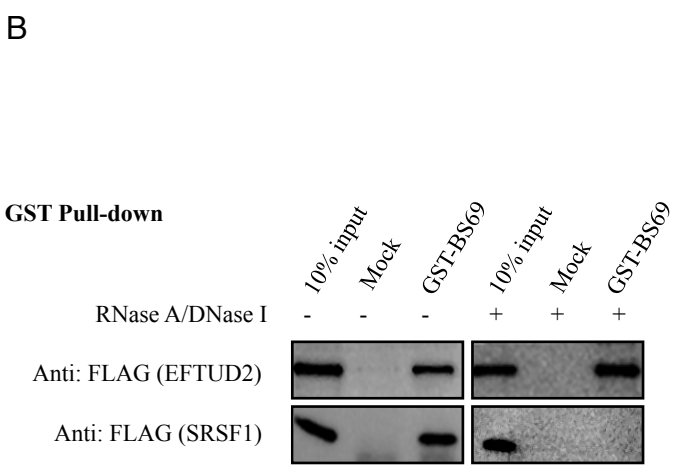
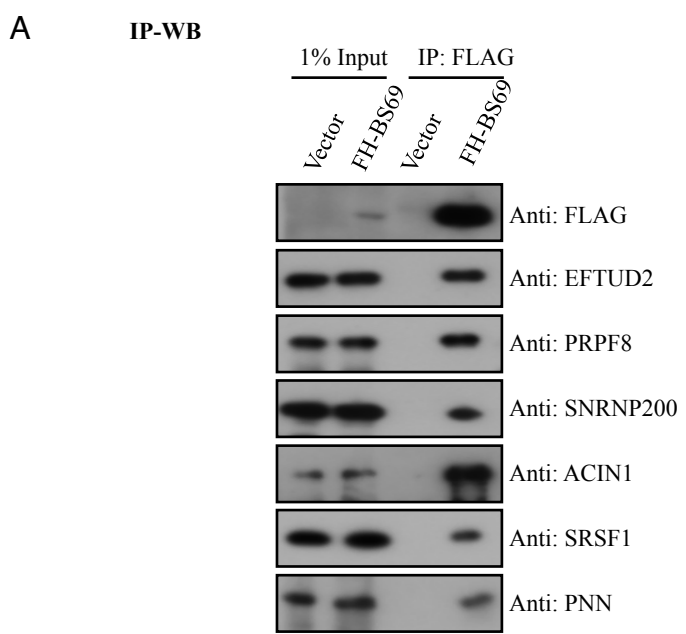
G

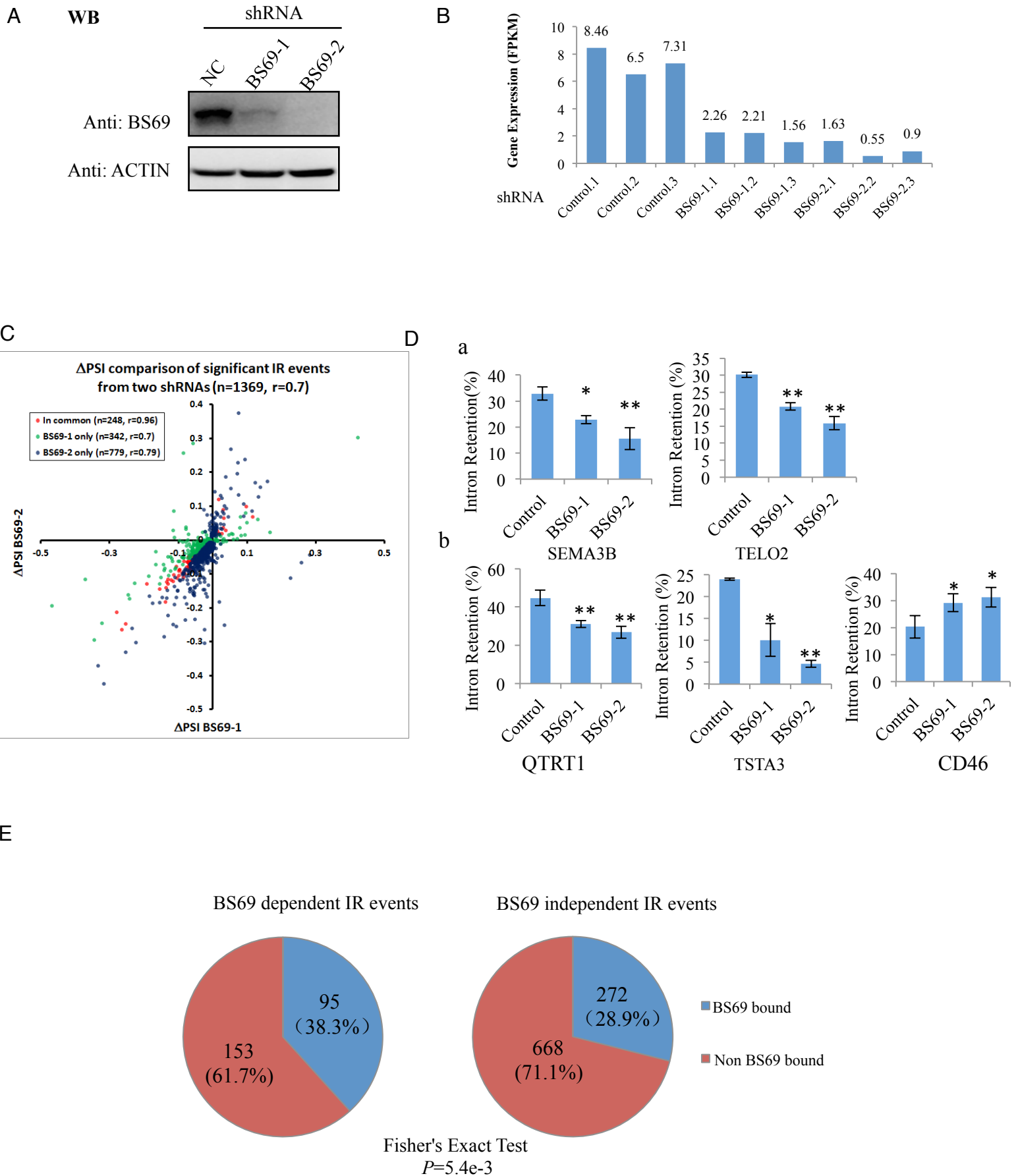
ChIP-qPCR:FLAG-BS69



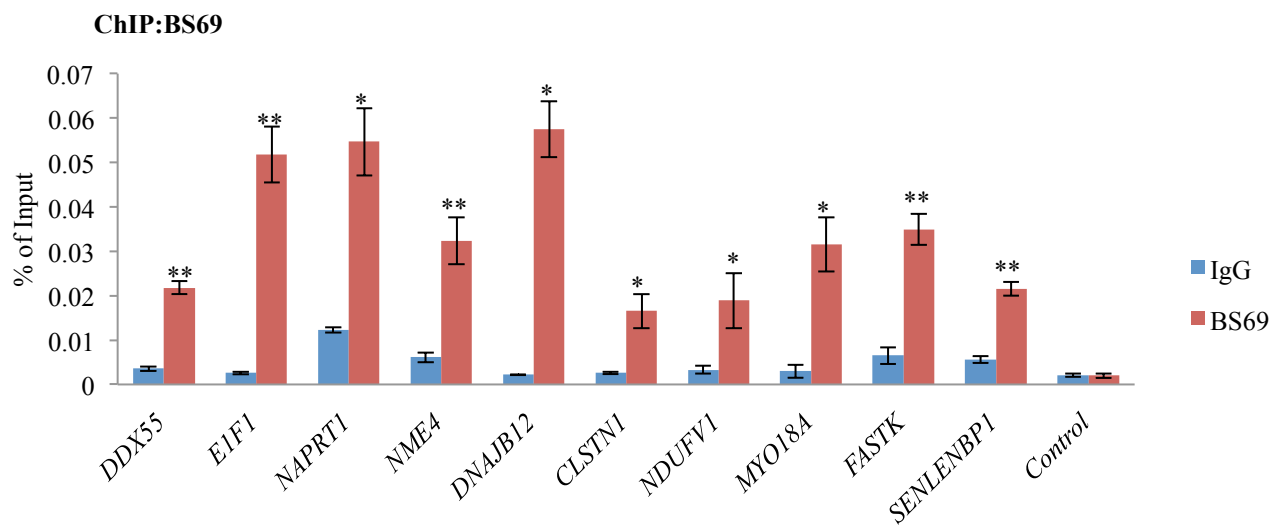
H



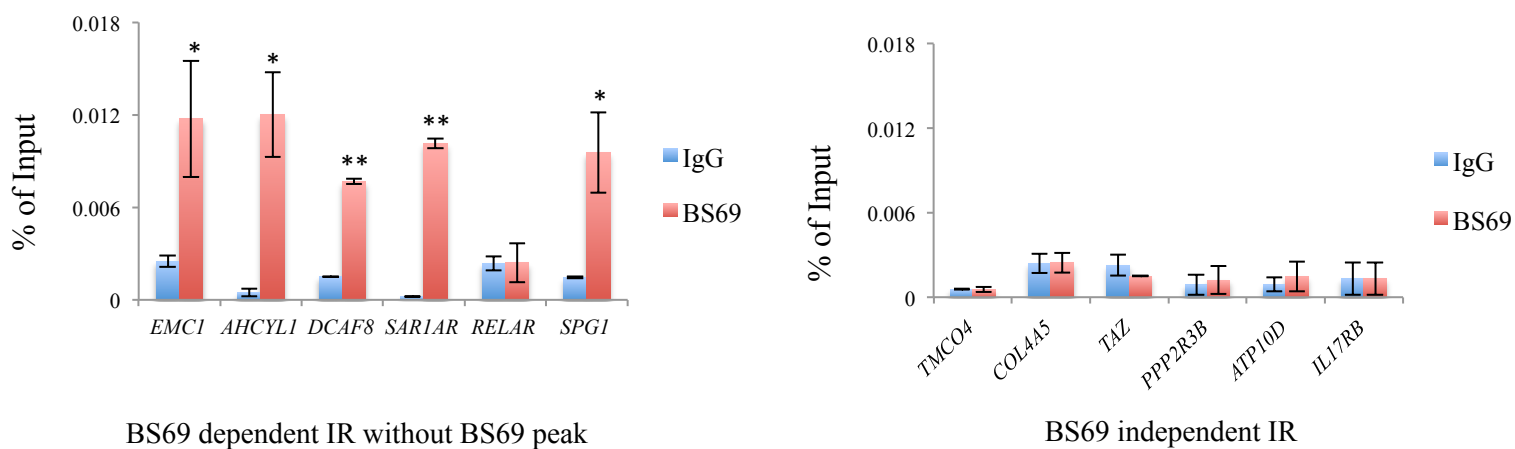




F



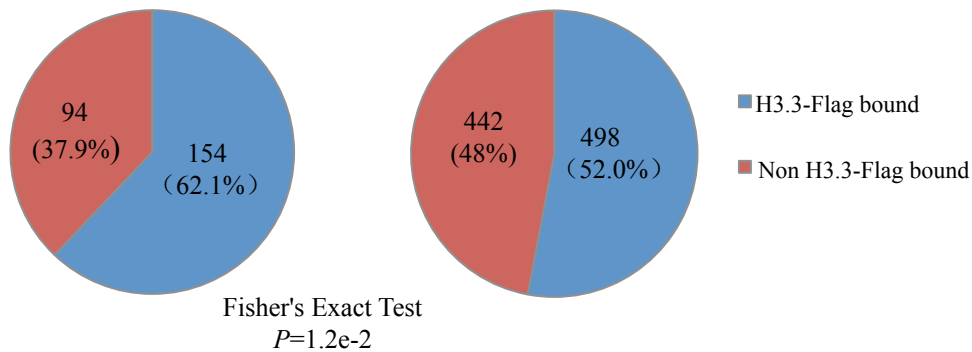
G



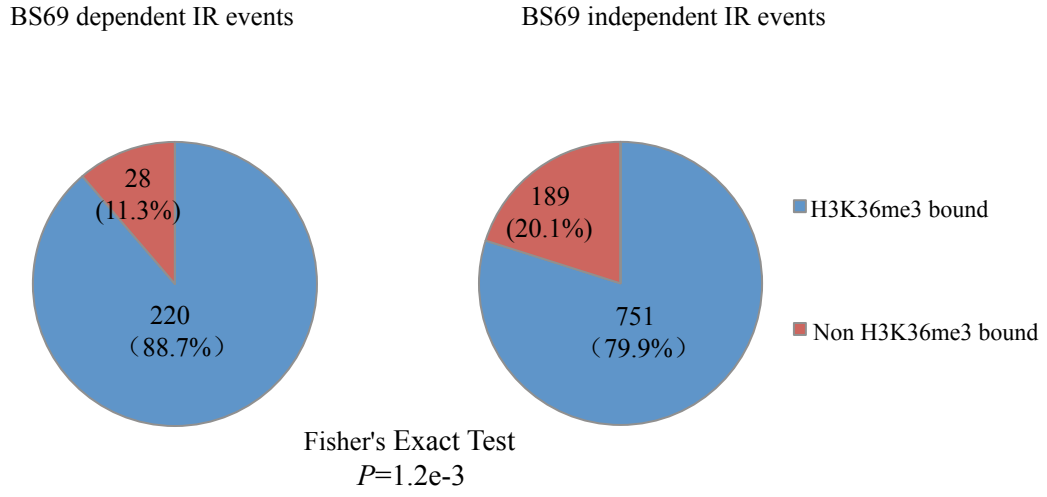
H

BS69 dependent IR events

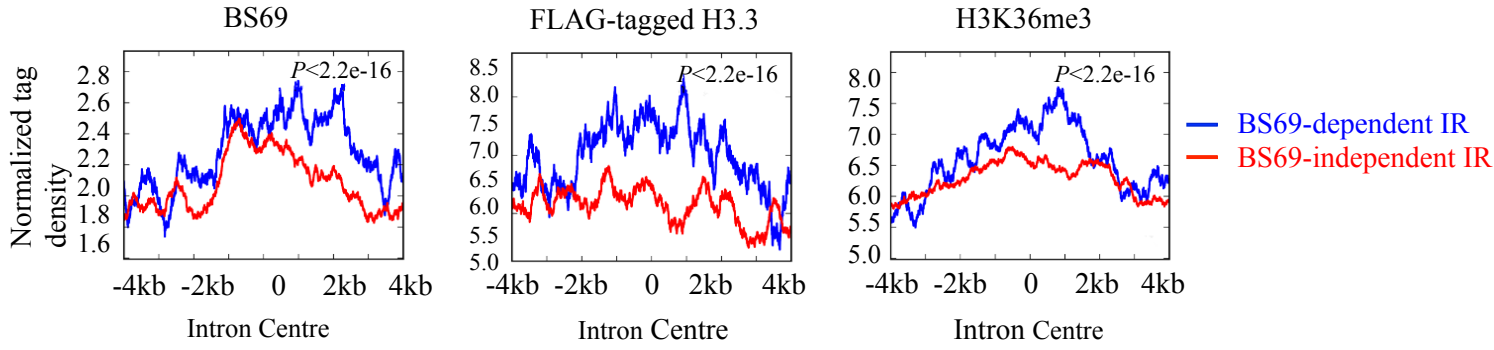
BS69 independent IR events



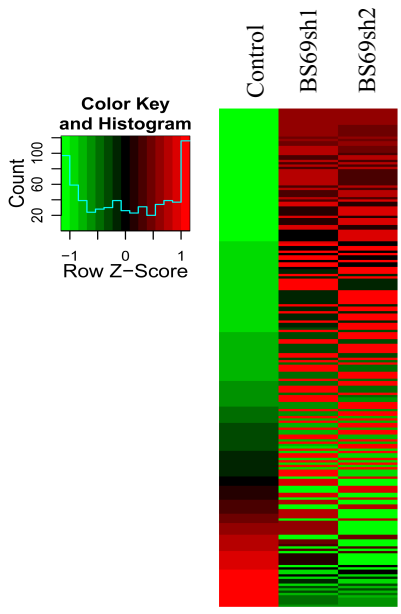
I



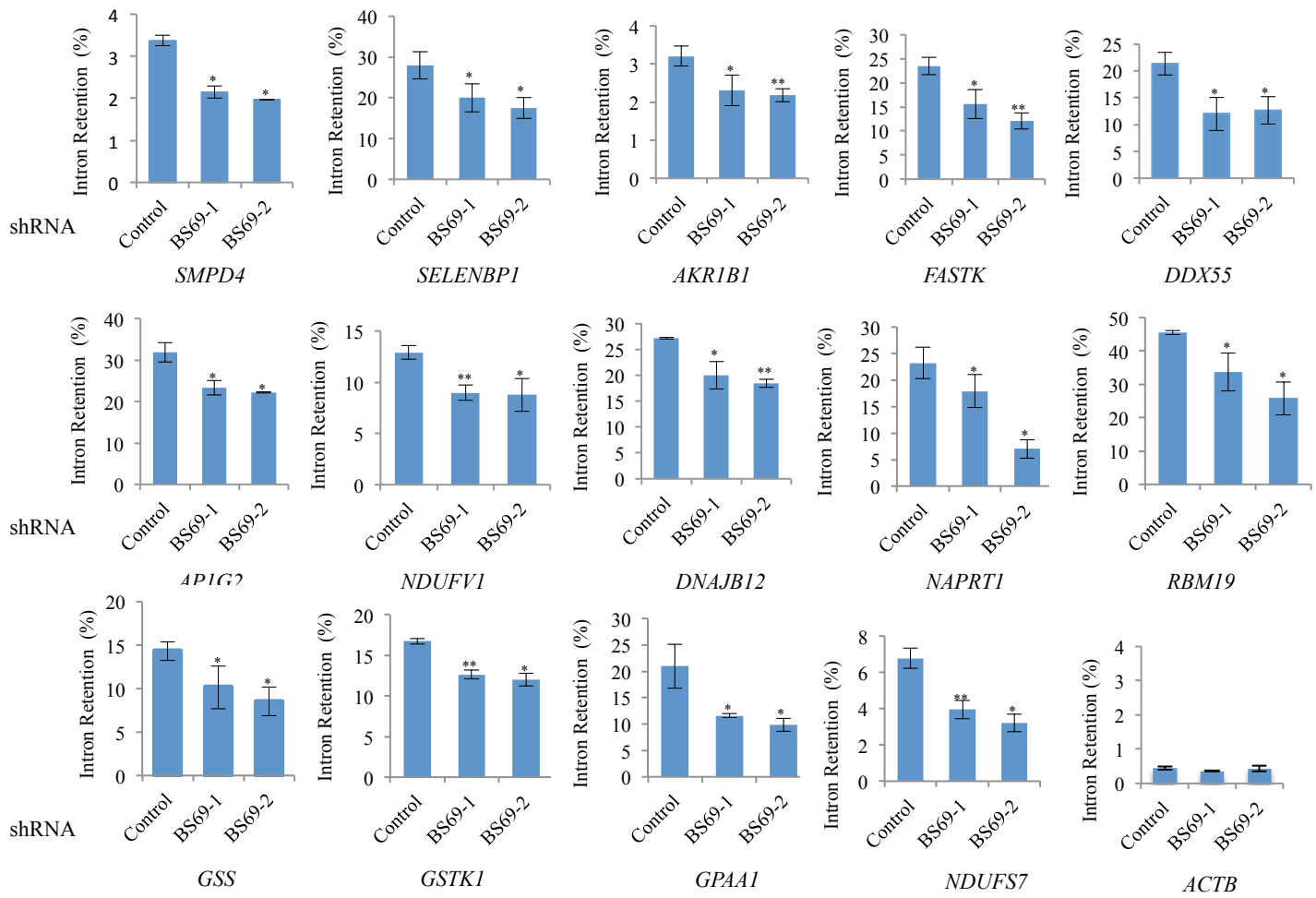
J



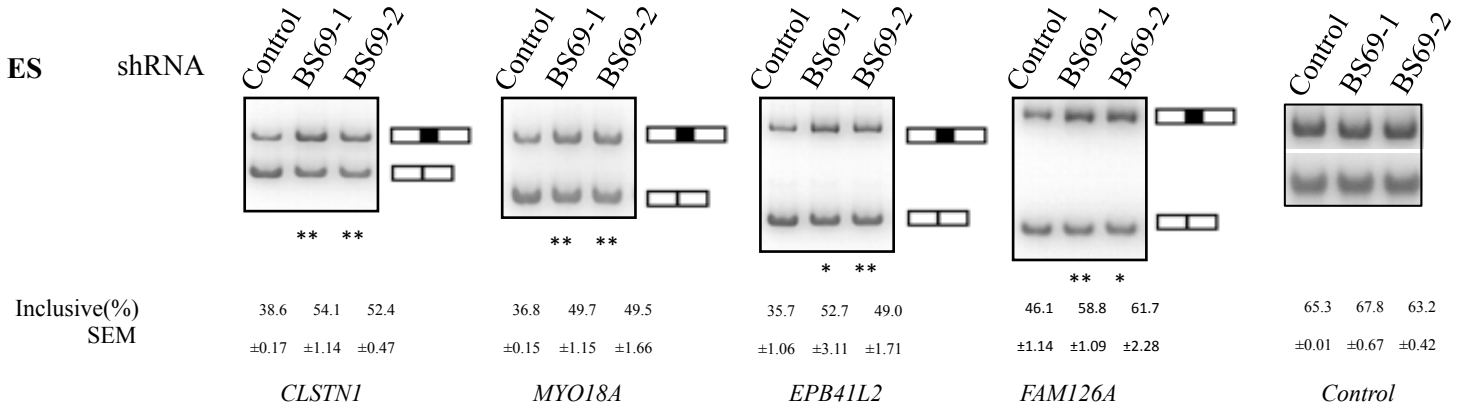
K



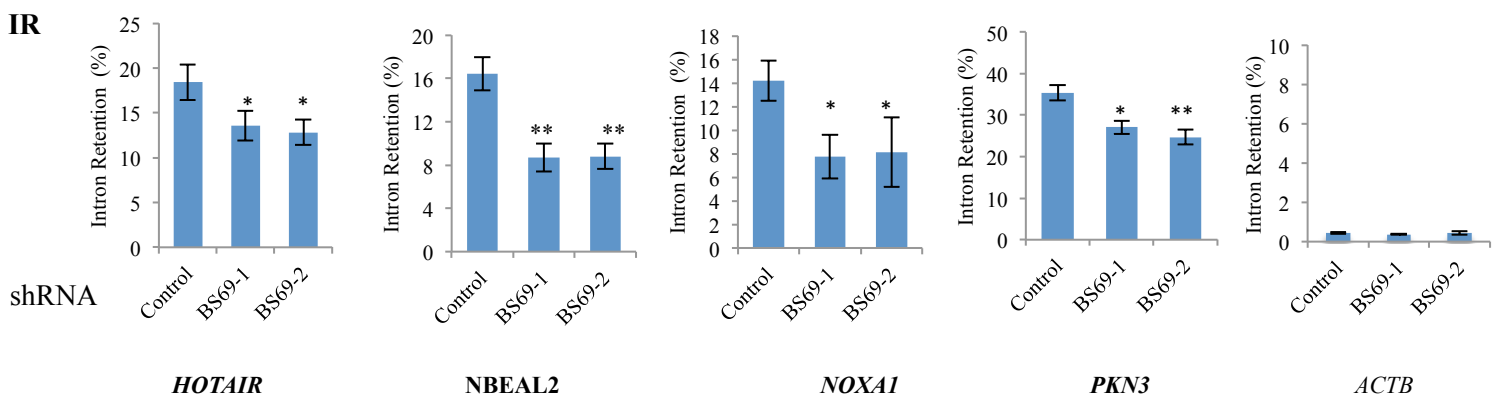
A IR



B

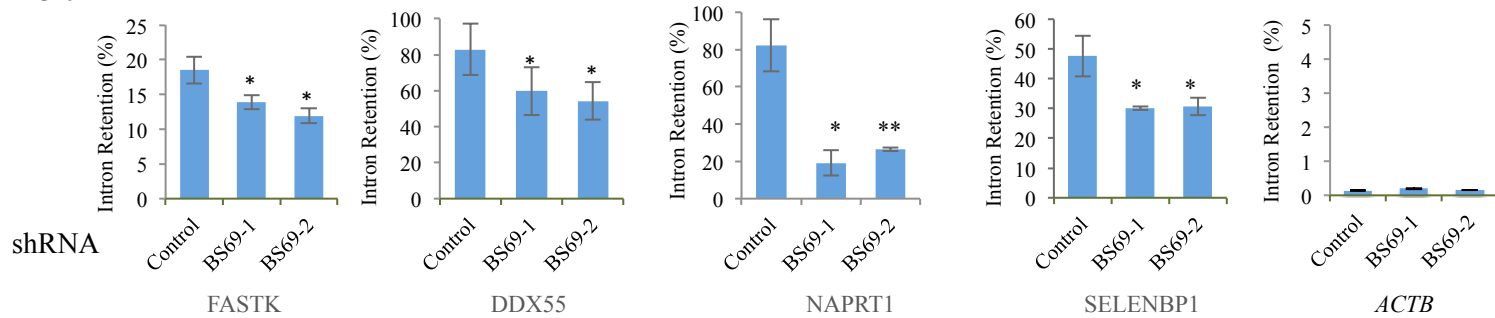


C

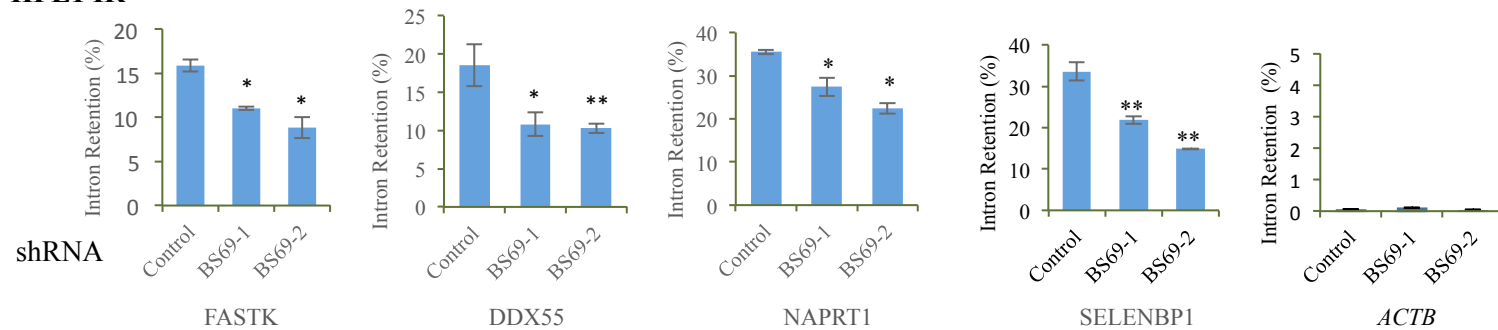


D

A549 IR



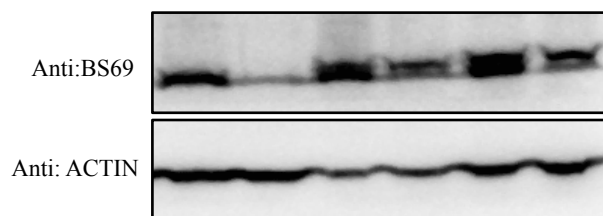
HFL1 IR



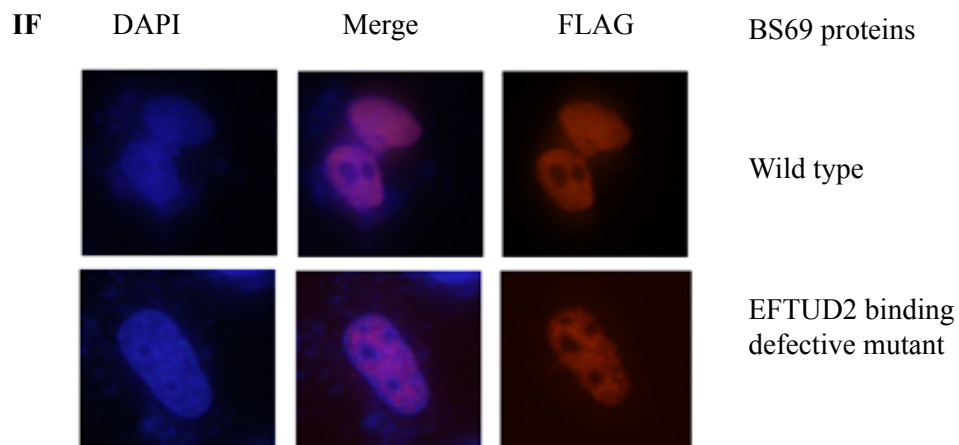
E

WB

Vector	+	+	-	-	-	-
BS69	-	-	+	+	-	-
BS69 Δ 556-562	-	-	-	-	+	+
Control shRNA	+	-	+	-	+	-
BS69 shRNA	-	+	-	+	-	+

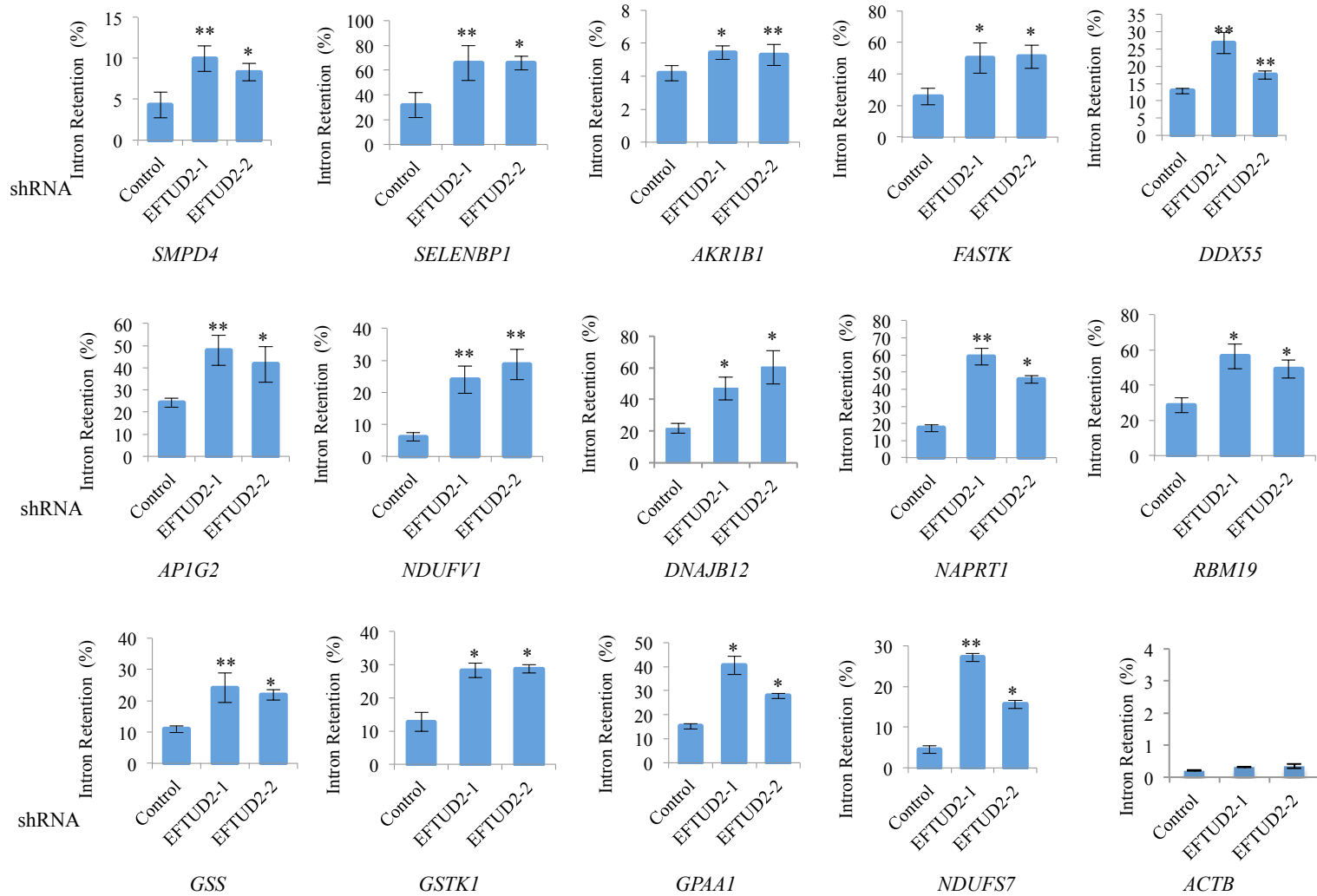


F



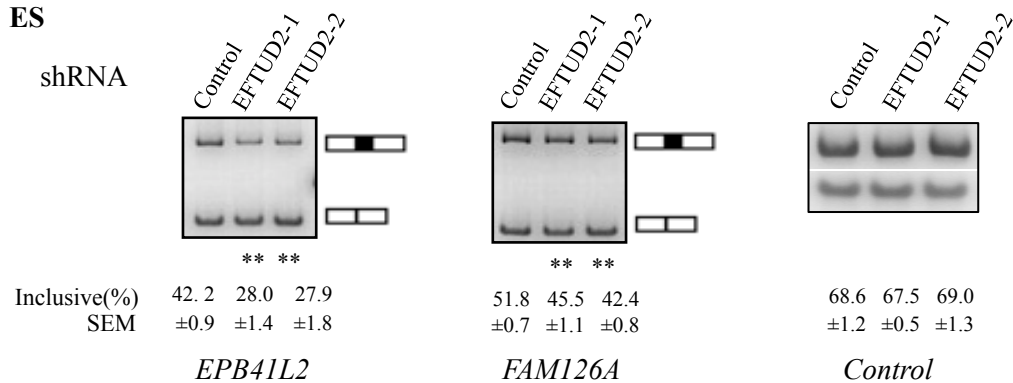
G

IR

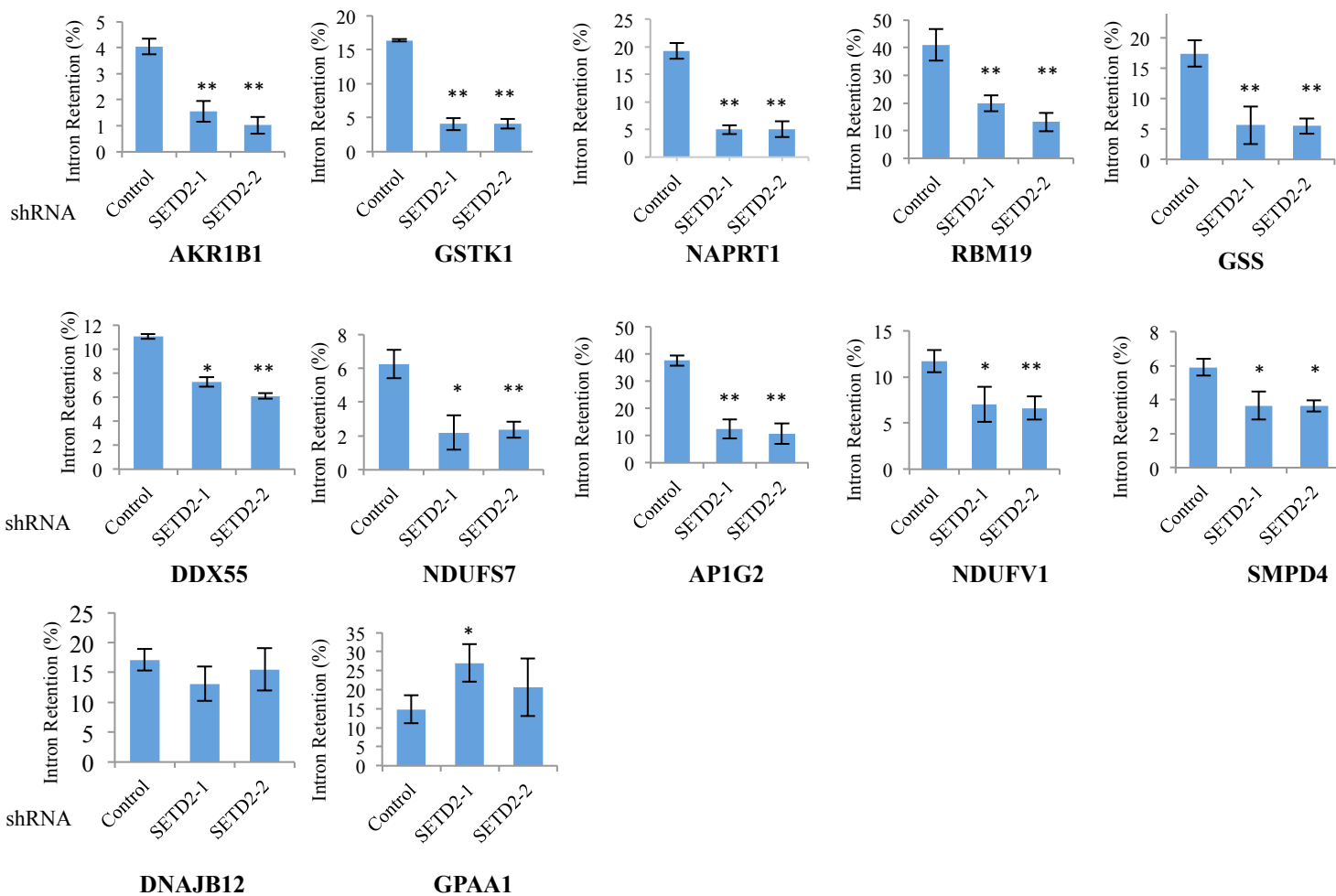


H

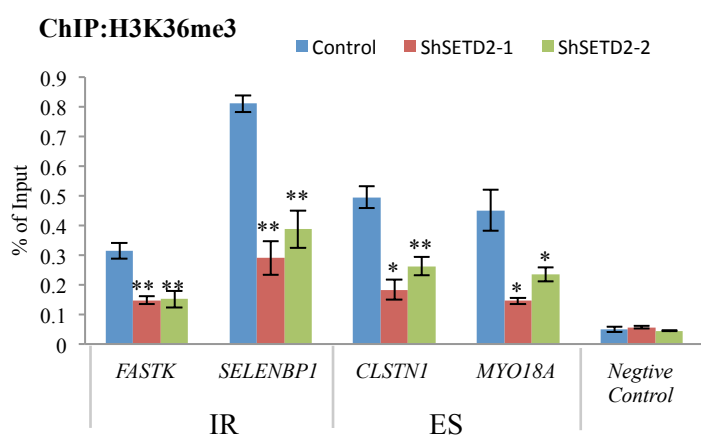
ES



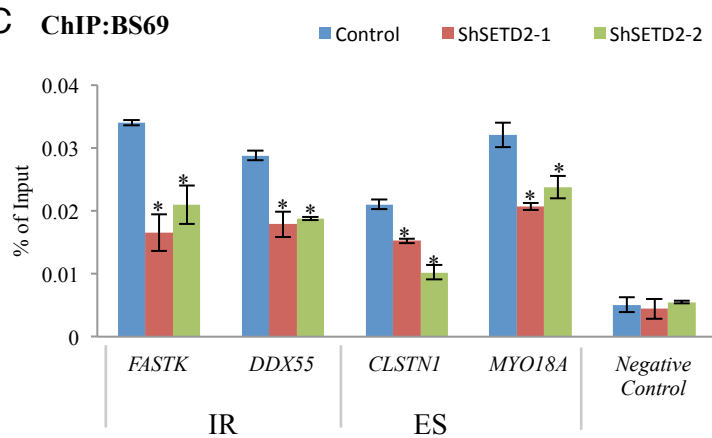
A



B

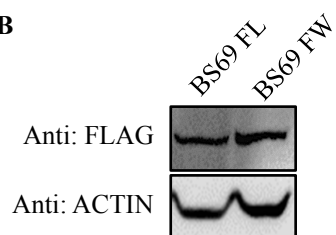


C



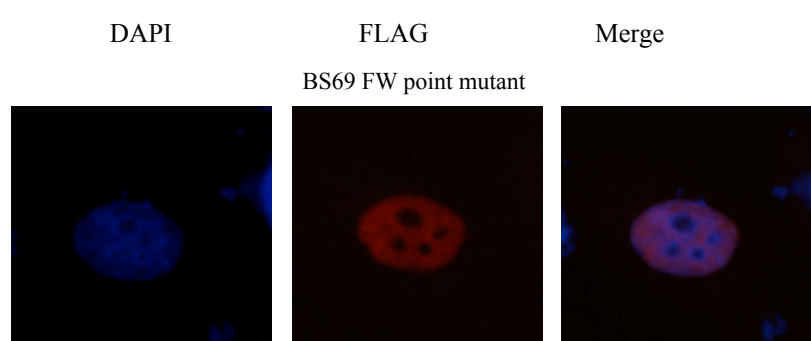
D

WB



E

IF



SUPPLEMENTAL FIGURE LEGENDS

Figure 1. BS69 shows a similar genomic distribution pattern as H3K36me3. Related to Figure 1.

Figure S1A. Genomic distribution of random peaks in HeLa cells.

Figure S1B. BS69 bound genes are significantly enriched for H3K36me3. *P*-value is calculated by hypergeometric test.

Figure S1C. BS69 co-localizes with H3K36me3 in gene bodies assessed by ChIP-qPCR. Primers for each gene were designed for the promoter (pro) and gene body (gb) regions, respectively. Data are represented as mean \pm SEM from 3 biological replicates, **P*<0.05, ***P*<0.01.

Figure S1D. H3K36me3 and BS69 levels in two independent SETD2 shRNA knockdown HeLa cells.

Figure 2. BS69 binds H3.3K36me3 in vitro via its PWWP domain. Related to Figure 2.

Figure S2A. GST tagged BS69 full length preferentially binds H3.3K36me3 in a histone peptide pull-down assay in vitro.

Figure S2B. Heatmap analysis of H3.3-FLAG and H3K36me3 distributions at BS69-bound TES regions. The TES regions are sorted by H3.3-FLAG ChIP-seq signal intensity. TESs are also grouped into “Plus strand” and “Minus strand” based on the orientation of transcription.

Figure S2C. Amino acid sequence alignment of the PWWP domains from human BS69, MSH6, DNMT3A, HDGF and WHSC1 proteins. Red arrows indicate the mutated amino acids, F and W, in the BS69 PWWP FW point mutant proteins used in this study.

Figure S2D. MST analyses of BS69₅₀₋₄₀₁ binding to various histone peptides. No detectable interaction between BS69₅₀₋₄₀₁ and the H3.1K36me3 (a), H3.1K36me0 (b) and H3.3K36me0(c) histone peptides, was observed in MST analyses.

Figure S2E. HA tagged BS69 full length protein purified from insect cells was used to bind HeLa nucleosome followed by histone H3 Western blot. Mock was performed using HA beads to inoculate with HeLa nucleosome in parallel. Immobilized BS69 protein was stained by Coomassie brilliant blue in the lower panel.

Figure S2F. Full length BS69 and the PWWP deletion mutant were expressed at comparable levels in HeLaS cells.

Figure S2G. Ectopically expressed wildtype BS69 but not the PHD and BROMO deletion mutants binds the selected BS69 targets (identified through endogenous BS69 ChIP) in HeLaS cells. Chromatin binding was determined by FLAG-ChIP and q-PCR. Data are represented as mean \pm SEM from 3 biological replicates, **P*<0.05, ***P*<0.01.

Figure S2H. MST analyses of BS69₅₀₋₄₀₁ binding to H3.3S31PK36me3. The K_d of BS69₅₀₋₄₀₁ binding to H3.3S31PK36me3 was determined to be 1540 \pm 43.6 μ M.

Figure 3. BS69 interacts with splicing factors. Related to Figure 3.

Figure S3A. The associations of splicing factors with FLAG-HA-BS69 were confirmed by FLAG IP followed by Western Blot analyses using indicated antibodies.

Figure S3B. The interactions between GST-BS69 and FLAG-EFTUD2 and FLAG-SRSF1 were verified by GST pull-down assay with or without RNase A/DNase I

treatment. Recombinant GST-BS69 was purified from *E.coli*, and recombinant FLAG-EFTUD2 and FLAG-SRSF1 were purified from Sf9 cells.

Figure S3C. Association of EFTUD2 with snRNAs. EFTUD2 was immunoprecipitated from HeLa cell extract using anti-EFTUD2 antibody and the associated RNA species were analyzed by RT-qPCR. Data are represented as mean \pm SEM from 3 biological replicates, * P <0.05, ** P <0.01; n.s., not significant.

Figure 4. BS69 regulates RNA splicing and induced NMD. Related to Figure 4.

Figure S4A. Two independent shRNAs effectively knocked down BS69 protein in HeLa cells.

Figure S4B. BS69 mRNA levels in the samples for RNA-seq analyses. Data from 3 biological replicates were shown.

Figure S4C. The correlation of the IR changes between two BS69 shRNAs analyzed by the scatterplot of the deltaPSI. The red dots are for 248 common events, green dots are for 342 events significant only in BS69-1, and blue dots are 779 events significant only in BS69-2.

Figure S4D: q-PCR confirmation of IR events affected by shRNA1 (a) or shRNA2 (b), respectively, but are not called by bioinformatics analysis (MATS: Multivariate Analysis of Transcript Splicing).

Figure S4E. BS69-dependent IR events are significantly enriched for BS69 binding.

Figure S4F. ChIP-qPCR confirmation of endogenous BS69 occupancies at 10 selected targets with altered AS upon BS69 KD. Data are represented mean \pm SEM from 3 biological replicates, * P <0.05, ** P <0.01.

Figure S4G: Left panel, BS69 binding events are identified at 5 out the 6 randomly selected IR events that regulated by BS69 KD by ChIP-q-PCR, but not identified by ChIP-seq. Right panel, in contrast, no BS69 binding was detected at another set of 6 randomly selected, BS69-independent IR sites by ChIP-q-PCR.

Figure S4H. BS69-dependent IR events are significantly enriched for H3.3-FLAG binding.

Figure S4I. BS69-dependent IR events are significantly enriched for H3K36me3 binding.

Figure S4J. ChIP-seq tag densities of BS69, H3K36me3 and H3.3-FLAG over introns that are BS69-dependent and BS69-independent. Significant differences of tag densities of all three factors were identified between BS69-dependent and -independent IR events. P -values were calculated using two-way unpaired Student's t -test.

Figure S4K. Heatmap analysis of the mRNA levels of 219 BS69 dependent IR genes identified from genome-wide intron survey.

Figure 5. BS69 regulates intron retention and exon skipping events by antagonizing EFTUD2 through physical interaction. Related to Figure 5.

Figure S5A. Knockdown of BS69 caused decreased intron retention (IR) of target genes in HeLa cells. Data are shown as mean \pm SEM from 3 biological replicates, * P <0.05, ** P <0.01.

Figure S5B. Knockdown of BS69 altered the ratio of exon skipping (ES) of target genes in HeLa cells. Data are shown as mean \pm SEM from 3 biological replicates, * P <0.05, ** P <0.01.

Figure S5C. Validation of 4 randomly chosen IR events identified from genome-wide intron survey in HeLa. Data are shown as mean \pm SEM from 3 biological replicates, * P <0.05, ** P <0.01.

Figure S5D. Knockdown of BS69 caused a decrease of IR in A549 and HFL1 cell lines. The target introns were selected based on our HeLa cell data. Data are shown as mean \pm SEM from 3 biological replicates, * P <0.05, ** P <0.01.

Figure S5E. Western blot analysis of BS69 protein levels in cells transfected with indicated constructs. BS69 RNAi-resistant rescue constructs directed BS69 expression in BS69 KD cells to a comparable level of the endogenous BS69.

Figure S5F. Both wildtype BS69 and EFTUD2 binding defective mutant (BS69 _{Δ 556-562}) showed nuclear localization when overexpressed in HeLa cells. M2 FLAG antibody was used in immunofluorescence assay to detect FLAG tagged BS69 proteins. Data shown are representatives of n=30 cells.

Figure S5G. Knockdown of EFTUD2 caused an increase in intron retention of BS69 target genes in HeLa cells. Data are shown as mean \pm SEM from 3 biological replicates, * P <0.05, ** P <0.01.

Figure S5H. Knockdown of EFTUD2 altered the ratio of exon skipping (ES) of target genes in HeLa cells. Data are shown as mean \pm SEM from 3 biological replicates, * P <0.05, ** P <0.01.

Figure 6. Binding H3K36me3 is important for BS69 to regulate AS. Related to Figure 6.

Figure S6A. Knockdown of SETD2 cause the alteration of intron retention (IR) of BS69 target genes in HeLa cells. Data are shown as mean \pm SEM from 3 biological replicates, * P <0.05, ** P <0.01.

Figure S6B and 6C. The occupancies of H3K36me3 and BS69 at selected genes with IR change were reduced in SETD2 shRNA treated HeLa cells. Data are shown as mean \pm SEM from 3 biological replicates, * P <0.05, ** P <0.01.

Figure S6D. The BS69 PWWP FW point mutant is expressed at a comparable level to that of the wildtype BS69 in HeLa cells.

Figure S6E. The BS69 PWWP FW point mutant showed nuclear localization when overexpressed in HeLa cells. M2 Flag antibody was used in immunofluorescence assay to detect FLAG tagged BS69 protein. Data shown are representatives of n=30 cells.

Protein Name	Peptide No.
Bait:BS69	40
SMARCA4/BRG1	9
SMARCC2	6
RIF1	19
MGA	83
MLL	20
PHC3	11
E2F6	7
ACIN1	13
L3MBTL2	14
RNF2	8
CBX4	6
BCORL1	11
KDM3B/JMJD1B	7
NSD1	5
SRRM2	31
SRRM1	7
PNN	10
SFRS4	8

Table S1. Polypeptides identified by tandem mass spectrometry from TAP purified BS69 complex from soluble HeLaS nuclear fraction without MNase treatment. Related to Figure 3.

Sample	Total Pairs	Mapped Pairs	%	Mapped Reads			
				Hg19	%	Splice Junction	%
CTRL-1	63,114,282	43,624,743	69.1%	56,045,791	44.4%	31,203,695	24.7%
CTRL-2	59,565,532	41,336,601	69.4%	52,979,144	44.5%	29,694,058	24.9%
CTRL-3	70,510,682	49,973,119	70.9%	64,286,170	45.6%	35,660,068	25.3%
CTRL total	193,190,496	134,934,463	69.8%	173,311,105	44.9%	96,557,821	25.0%
BS69-1.1	69,493,586	49,538,807	71.3%	63,468,350	45.7%	35,609,264	25.6%
BS69-1.2	64,182,964	44,364,888	69.1%	56,612,938	44.1%	32,116,838	25.0%
BS69-1.3	65,830,993	45,731,865	69.5%	58,323,903	44.3%	33,139,827	25.2%
BS69-1 total	199,507,543	139,635,560	70.0%	178,405,191	44.7%	100,865,929	25.3%
BS69-2.1	68,664,446	48,495,946	70.6%	61,244,443	44.6%	35,747,449	26.0%
BS69-2.2	73,231,810	52,125,572	71.2%	66,579,173	45.5%	37,671,971	25.7%
BS69-2.3	62,620,747	44,591,595	71.2%	56,801,434	45.4%	32,381,756	25.9%
BS69-2 total	204,517,003	145,213,113	71.0%	184,625,050	45.1%	105,801,176	25.9%
Total	597,215,042	419,783,136	70.3%	536,341,346	44.9%	303,224,926	25.4%

Table S2. Mapping Statistics of BS69 RNA-seq data. A total of 597 million pairs (199M BS69-1.KD, 204M BS69-2.KD, 193M CTRL) were mapped. Sequencing mode: 100bp paired-end read, 25bp seed, 2 bp mismatch per seed allowed, anchor Length 8bp. Related to Figure 4.

Table S3. List of DNA oligonucleotides used in this study. Related to Figure 1, 2, 3, 4, 5 and 6.

Name	Sequence	Name	Sequence
EFHD2-F pro	TGAAACCCAGTCCCATCTCC	NUP188-F	CCACTTCACCCCAGATGTCT
EFHD2-R pro	CACTGGCGTTCTCAATGAGG	NUP188-R	ACAGCAGAGCAGAGCCTTTA
EFHD2-F gb	CGAGATTGGGAGAGCAGGAT	DDX39-F	TGCGGTTCTTCTCACTGTCT
EFHD2-R gb	ACCCAGGAGCATTACAGTTA	DDX39-R	CATGGAGGTGTTTGTGGACG
SLC7A5-F pro	TTATGAGTCAGCCCGTGTCA	ANXA2-F	TTCCGTATTATCCGCCACA
SLC7A5-R pro	CAATACTCCAGCCTCTTGC	ANXA2-R	GAATGCCTATCGTGTGCCAG
SLC7A5-F gb	AGCTCACTCTCCACAAGGA	SAP30BP-F	GAGACTCGGCTACTGAGGTC
SLC7A5-R gb	TCAGCTTCAGAGGGTCTGGT	SAP30BP-R	AGAAGCCTCAGTCCCTTTCC
DAXX-F pro	AGAGGTTCCCTCCCAACAGT	ITPR3-F	CGAGTACCTGAGCATCGAGT
DAXX-R pro	GTTACGGGTCACCGAGAGAA	ITPR3-R	AGCTGCCTCACACTCTTCTC
DAXX-F gb	CGCCTGTTAACCTCTGGGTA	ZBTB7A-F pro	CCTGGTCCAGTTCTGAGGTT
DAXX-R gb	ATGACCCAGACTCCGCATAC	ZBTB7A-R pro	CCACTAAATGTTGGCGGAAT
ZFP36L2-F	AGCCGATGGTATGAAAGGTG	ZBTB7A-F gb	GACCCACCTGAGTGACCT
ZFP36L2-R	AGATCAACTCCACGCGCTAC	ZBTB7A-R gb	TGCCATATGAGGAGGAAACC
LAMA5-F	GACGCTGAAAGCACAAACAA	TAF2-F pro	CTGAGCCTGGGTGAAAAGTC
LAMA5-R	GCCTGGAGTACAACGAGGTC	TAF2-R pro	TTTCTCGGCTCTACCTTCCA
EEF2-F	AACCAGGGGAAAGAGACGTT	TAF2-F gb	AGGCCTTCCCAGATAATGCT
EEF2-R	TCACTGATACCCGGAAGGAC	TAF2-R gb	CTCCGTCTCTTCTCCACAG
PLEC-F	CGTCAGCGATGTCATCATT	CLSTN1 F ES	ACGAGCCCTTCTCTGTGACT
PLEC-R	TCCAGATTGCCCTGGACTAC	CLSTN1 R ES	AAACTGGGTCATGTGCAGGT
RPLB-F	GAGGCTGAGTTCATCACAA	MYO18A F ES	CTCCGAGTCCACATCAGAGT
RPLB-R	TGCTGTTGAGGCGTTAAATG	MYO18A R ES	GCCATTGAGGATGAGATGGA
GPX4-F	AGATCCACGAATGTCCCAAG	EBP41L2 F ES	CTCTTTCGTCTTTCCCAACC
GPX4-R	AAGACCTGAACGCTCCTCCT	EBP41L2 R ES	GTGAGAAGCCCAACTAAAGC
TVAS4-F	TGCATTGTGAGATGCGAAAT	FAM126A F ES	GCAGCCCTGGAATAAAAATCC
TVAS4-R	CTTTAAGTGGCTGCCTTTGC	FAM126A R ES	CCAGCATGTCAATAAGGGGT
EEF1G-R	TGTAGGACGCTGAGTGCTTG	SELENBP R M IR	CAAGGGGAGTGCTGAAATCCA
CCNL2-F	TTCAGACCAAAGGGAGGTG	SELENBP F S IR	CTGATCATCACTTCCCCGCT
CCNL2-R	TTCTCCTGCACTTCATTCC	SELENBP R S IR	AAGTGCGAACCTGGCCTTTCT
GAPDH-F	GGCTCATTGTCAGGGGGGAG	FASTK F M IR	CCGGCACCTCATCTAATCT
GAPDH-R	AGGGGCCATCCACAGTCTTC	FASTK R M IR	TCGGCCACCATAAACTGGG
U1-F	GGGGAGATAACCATGATCACG	FASTK F S IR	TAAACTGCTGTTCCAGGGGC
U1-R	GTCGAGTTTCCCACATTTGG	FASTK R S IR	AGAAGTTGGTCTGCCCTTT
U2-F	GGCCTTTTGGCTAAGATCAAG		
U2-R	TGGAGGTAAGTCAATACCAGG		
U4-F	ATGAGGTTTATCCGAGGCG		
U4-R	CGTAGAGACTGTCAAAAATTGCC		
U5-F	ATACTCTGGTTTCTTTCAGATCG		
U5-R	TGGTTAAGACTCAGAGTTGTTCC		
U6-F	TGGAACGATACAGAGAAGATTAGC		
U6-R	GAACGCTTCACGAATTTGC		

SUPPLEMENTARY EXPERIMENTAL PROCEDURES

Cell culture and reagents

HeLa, HEK293T, HFL-1 and A549 cells were obtained from ATCC, and maintained according to ATCC instructions. Two BS69 antibodies were raised in rabbits against His-BS69 (1-92aa) and synthetic peptide (47-52aa), respectively. Other antibodies used for Western blotting and immunoprecipitation include: ACTIN (Abmart, P30002), FLAG (Abmart, M20008M; Sigma, Clone M2), HA (Santa Cruz Bio., sc-7392), SNRNP200 (Bethyl, A303-454A), EFTUD2 (Bethyl, A300-957A), PRPF8 (Sigma, ab79237), Histone H3 (Abcam, ab1791), Histone H3K36me3 (Active Motif, 61101), SRSF1 (Epitomics, #5764-1), ACIN1 (Bethyl, A300-999A), PNN (A301-022A). Modified histone peptides were synthesized by Beijing Scilight Biotechnology LLC.

In Vitro Binding and co-immunoprecipitation assays

For peptide pull-down assays, purified, 2 µg full length and N-terminal recombinant GST-BS69 proteins were incubated with 2 µg of various biotinylated histone peptides in the binding buffer (50 mM Tris-HCl pH 7.4, 200 mM NaCl, 0.2% NP-40, 1 mM MgCl₂, 5% Glycerol) at 4°C for 2 hours. The protein-peptide complexes were immobilized to streptavidin beads at 4°C for 1 hour. The streptavidin beads were washed 5 times with binding buffer and the bound proteins were separated on 10% SDS-PAGE followed by Coomassie Blue staining.

For nucleosome binding assays, 2 µg of full length GST-BS69 were immobilized on GST resins first, which were then incubated with 2 µg HeLaS nucleosome in the binding buffer (50 mM Tris-HCl pH 7.4, 200 mM NaCl, 0.2% NP-40, 1 mM MgCl₂, 5% Glycerol) at 4°C for 4 hours. After 5 washes with binding buffer, the bound proteins were separated on 10% SDS-PAGE followed by Western blotting using a histone H3 antibody. For protein-protein interaction assays described in Figure S2b, FLAG-SRSF1 and FLAG-EFTUD2 were purified from insect cells, and GST-tagged BS69 proteins were purified from *E.coli* and immobilized on GST resins before incubation. 2 µg FLAG tagged and 2 µg GST tagged proteins were used in the pull-down assay, which was performed as described above in the nucleosome-binding assay.

Immunoprecipitation

Nuclear extracts were prepared from HeLa cells as described before (Mendez and Stillman, 2000) with the following modifications. Micrococcal nuclease (MNase) (Sigma) was added to nuclear extract at 37°C for 3 min, and then lysate was centrifuged at 12,000 rpm for 10 min at 4°C. Supernatant was incubated with 5 µg BS69 antibody or IgG followed by the addition of 20 µl of Protein A/G agarose beads (Santa Cruz). After overnight incubation at 4°C, beads were washed 5 times with washing buffer (50 mM Tris-HCl pH 7.9, 150 mM KCl, 5 mM MgCl₂, 0.2 mM EDTA, 20% glycerol, 0.1% NP-40, 3 mM β-ME, protease inhibitors), and boiled for 10 min in 50 µl of SDS loading buffer for Western blotting analysis.

BS69 protein complex tandem affinity purification and reciprocal immunoprecipitation

Tandem affinity purification was performed as described previously (Ogawa et al., 2002) with some minor modifications. In brief, FLAG-HA-BS69 stably expressing HeLaS cells was established using a retroviral expressing system. HeLaS nuclear extract was treated with MNase at 37°C for 3 min followed by centrifugation at 12000 rpm for 10 min at 4°C. Treated nuclear extract was then incubated with anti-FLAG M2 agarose (Sigma) in the binding buffer (50 mM Tris-HCl pH 7.9, 150 mM KCl, 5 mM MgCl₂, 0.2 mM EDTA, 20% glycerol, 0.1% NP-40, 3 mM β-ME, protease inhibitors) for 6 hours, and then washed with the same buffer and eluted with FLAG peptides (Sigma). The FLAG elution was then incubated with anti-HA beads (Sant-cruz Biotechnology). After washing (3X), the bound proteins were eluted with HA peptides (Covance). The purified protein complex was subjected to MS-MS analysis. For reciprocal immunoprecipitation in Figure 2b, FLAG-purified BS69 complex was precipitated using either anti-EFTUD2 or IgG antibody. The immunoprecipitants were analyzed by Western blotting using corresponding antibodies.

snRNA Association analyses

HeLa cells transfected with FLAG-BS69 plasmid grown in 150 cm plates were covered with ice-cold PBS buffer and subjected to UV-irradiation (150 mJ/cm²) for crosslinking (Konig et al., 2010). Lysis buffer (50 mM Tris-HCl, pH7.4; 100 mM NaCl; 1% NP-40; 0.1% SDS; 0.5% Na-deoxycholate; 1/1000 protease inhibitor cocktail, Roche) was added to cell pellets. Cell lysate was cleared by centrifugation at 12,000 rpm and 4°C for 10 min, and then incubated with 20 µl of FLAG beads per ml of cell lysate at 4°C for 2 hours. After incubation, the FLAG beads were washed twice with the high-salt buffer (50 mM Tris-HCl, pH7.4; 1 M NaCl; 1 mM EDTA; 1% NP-40; 0.1% SDS; 0.5% Na-deoxycholate) and twice with the low salt buffer (20 mM Tris-HCl, pH7.4; 10 mM MgCl₂; 0.2% Tween-20). The bound RNA-protein complex was extracted by phenol-chloroform. In Figure 2g, the recovered RNA was separated by 8% urea denaturing gel, transferred onto nylon membrane (Hybond N, GE Healthcare) and hybridized with digoxigenin-labeled specific DNA probes for U1, U2, U4, U5 and U6 (PCR-labeling Mix kit from Roche) and then detected by CSPD (Roche). In Figure 2h, the recovered RNA was examined by RT-qPCR using U1, U2, U4, U5 and U6 snRNA primers.

Chromatin immunoprecipitation (ChIP) and ChIP-seq

ChIP assays were carried out as previously described (Lan et al., 2007) with some modifications of buffer compositions. Briefly, chromatin samples were incubated with specific antibodies in the ChIP Lysis buffer (50 mM HEPES pH7.5, 500 mM NaCl, 1 mM EDTA, 1% Triton, 0.1% Na-deoxycholate, 0.3% SDS) overnight at 4°C. The protein-DNA complexes were immobilized on protein A/G beads (10 µl per reaction). The bound fractions were washed 3 times with the lysis buffer, and 3 times with RIPA buffer (50 mM HEPES, 300 mM LiCl, 1 mM EDTA, 0.5% NP-40, 0.7% Na-deoxycholate), and once with TE. Elution and reverse crosslinking were carried out in the elution buffer (50 mM Tris-HCl PH8.0, 10 mM EDTA, 1% SDS) 65°C for 6 hours. After RNase A and Proteinase K digestion, DNA was purified using PCR extraction kit (QIAGEN).

RNA-seq bioinformatics analysis

We mapped RNA-seq reads to human transcripts (Ensembl, release 65) and genome (hg19) using the software TopHat(Trapnell et al., 2009) allowing 2bp mismatches per 25bp seed. We used MATS(Shen et al., 2012) ([http://rnaseq-mats.sourceforge.net/; version 3.0.7](http://rnaseq-mats.sourceforge.net/;version 3.0.7)) to identify BS69-regulated differential alternative splicing events corresponding to all five types of alternative splicing patterns. Briefly, MATS uses a modified version of the generalized linear mixed model to detect differential alternative splicing from RNA-seq data with replicates. It accounts for exon-specific sequencing coverage in individual samples as well as variation in exon splicing levels among replicates. Putative BS69-regulated alternative splicing events were identified as those with significant difference in inclusion levels between knockdown and control, at FDR<10%. To test if BS69-dependent IR events are enriched for specific genomic features (Figure S4E, S4H-J), we compiled a high-confidence set of BS69-independent IR events, using the criteria of FPKM (RNA-seq gene expression level) > 5 and IR level >5% in either the control or BS69 KD samples (MATS FDR>95%).

Statistical analyses

All the P-values in Figure 1E, 1F, 2C, 2G, 3H, 4C, 5A, 5B, 5D, 5E, 6A-D and Figure S1C,2G, 3C, 4D, 4F, 4G,5A-D, 5G, 5H, 6A, 6B, 6C were calculated by two-sided t-test. All the P-values in Figure 4E, 4H and 4I were calculated by two-sided Fisher's exact test. P-value in Figure S1B was calculated by hypergeometric test. P-values in Figure 1A and S1A were calculated by binomial test. S4J was calculated by two-way unpaired Student's t-test.

SUPPLEMENTAL REFERENCES

- Konig, J., Zarnack, K., Rot, G., Curk, T., Kayikci, M., Zupan, B., Turner, D.J., Luscombe, N.M., and Ule, J. (2010). iCLIP reveals the function of hnRNP particles in splicing at individual nucleotide resolution. *Nature structural & molecular biology* *17*, 909-915.
- Lan, F., Bayliss, P.E., Rinn, J.L., Whetstine, J.R., Wang, J.K., Chen, S., Iwase, S., Alpatov, R., Issaeva, I., Canaani, E., *et al.* (2007). A histone H3 lysine 27 demethylase regulates animal posterior development. *Nature* *449*, 689-694.
- Mendez, J., and Stillman, B. (2000). Chromatin association of human origin recognition complex, cdc6, and minichromosome maintenance proteins during the cell cycle: assembly of prereplication complexes in late mitosis. *Mol Cell Biol* *20*, 8602-8612.
- Ogawa, H., Ishiguro, K., Gaubatz, S., Livingston, D.M., and Nakatani, Y. (2002). A complex with chromatin modifiers that occupies E2F- and Myc-responsive genes in G0 cells. *Science* *296*, 1132-1136.
- Shen, S., Park, J.W., Huang, J., Dittmar, K.A., Lu, Z.X., Zhou, Q., Carstens, R.P., and Xing, Y. (2012). MATS: a Bayesian framework for flexible detection of differential alternative splicing from RNA-Seq data. *Nucleic acids research* *40*, e61.
- Trapnell, C., Pachter, L., and Salzberg, S.L. (2009). TopHat: discovering splice junctions with RNA-Seq. *Bioinformatics* *25*, 1105-1111.